The integrator complex is required for integrity of Cajal bodies

Hideaki Takata[1,2,*], Hitoshi Nishijima[1,3,4], Kazuhiro Maeshima[2,3] and Kei-ichi Shibahara[1,3,*]

[1]Department of Integrated Genetics, National Institute of Genetics, Research Organization of Information and Systems, Mishima 411-8540, Japan
[2]Structural Biology Center, National Institute of Genetics, Research Organization of Information and Systems, Mishima 411-8540, Japan
[3]Department of Genetics, School of Life Science, The Graduate University for Advanced Studies, Mishima 411-8540, Japan
[4]Division of Molecular Immunology, Institute for Enzyme Research, University of Tokushima, Tokushima 770-8503, Japan

*Authors for correspondence (htakata@lab.nig.ac.jp; kshibaha@lab.nig.ac.jp)

Accepted 20 July 2011
Journal of Cell Science 125, 166–175
© 2012. Published by The Company of Biologists Ltd
doi: 10.1242/jcs.090837

Summary

The nucleus in eukaryotic cells is a highly organized and dynamic structure containing numerous subnuclear bodies. The morphological appearance of nuclear bodies seems to be a reflection of ongoing functions, such as DNA replication, transcription, repair, RNA processing and RNA transport. The integrator complex mediates processing of small nuclear RNA (snRNA), so it might play a role in nuclear body formation. Here, we show that the integrator complex is essential for integrity of the Cajal body. Depletion of INTS4, an integrator complex subunit, abrogated 3′-end processing of snRNA. A defect in this activity caused a significant accumulation of the Cajal body marker protein coilin in nucleoli. Some fractions of coilin still formed nucleoplasmic foci; however, they were free of other Cajal body components, such as survival of motor neuron protein (SMN), Sm proteins and snRNAs. SMN and Sm proteins formed striking cytoplasmic granules. These findings demonstrate that the integrator complex is essential for snRNA maturation and Cajal body homeostasis.

Key words: Cajal body, Integrator complex, snRNP maturation

Introduction

The eukaryotic nucleus is a functionally compartmentalized structure characterized by various nuclear bodies, domains and chromosome territories (Lamond and Earnshaw, 1998; Cremer et al., 2006; Zhao et al., 2009). Nuclear bodies are typically enriched for specific proteins and nucleic acids to specify and facilitate their functions (Misteli, 2007). However, little is known about how these nuclear bodies are organized. The understanding of this process is an important issue in cell biology.

One of the prominent nuclear bodies is the Cajal body (also known as the ‘coiled body’). Cajal bodies were first described in vertebrate neurons in 1903 by Ramón y Cajal (Cajal, 1903). They are conserved structures found in both animals and plants, but the size and number of Cajal bodies vary, depending on many factors, including cell type, cell cycle stage and metabolic activity (Beven et al., 1995; Gall, 2000; Cioce and Lamond, 2005). Cajal bodies contain small nuclear ribonucleoprotein particles (snRNPs) and small nucleolar ribonucleoprotein particles (snoRNPs), which are essential factors for pre-mRNA splicing and ribosomal RNA processing, respectively. Cajal bodies also contain a range of proteins including coilin, a protein essential for Cajal body formation, and some nucleolar proteins such as fibrillarin, dyskerin and Nopp140 (Ogg and Lamond, 2002; Cioce and Lamond, 2005; Matera and Shpargel, 2006). Newly assembled snRNPs and snoRNPs are generally assumed to traffic through Cajal bodies before accumulating in the nuclear speckles and nucleoli, respectively. Thus, Cajal bodies might be involved in maturation of snRNPs and snoRNPs (Sleeman and Lamond, 1999; Sleeman et al., 2001).

The mechanism of Cajal body formation remains unclear, but recent studies suggest that they are formed by the ‘self-organization’ of Cajal body components, reflecting uridine (U)-rich snRNP biogenesis (Lemm et al., 2006; Kaiser et al., 2008; Shevtsov and Dundr, 2011). In vertebrates, U1, U2, U4 and U5 snRNA genes are transcribed by RNA polymerase II (RNA pol II) and modified to carry a 5′-terminal 7-monomethylguanosine (m_7G) cap structure and short non-polyadenylated 3′-elongated sequences (Huang et al., 1997). Such modified snRNA precursors are exported to the cytoplasm by an export complex (Ohno et al., 2000). In the cytoplasm, the survival of motor neuron protein (SMN) complex (Kolb et al., 2007) facilitates the assembly of Sm proteins on the snRNAs (Raker et al., 1996). This is followed by hypermethylation of the 5′-cap [2,2,7-trimethylguanosine (m_3G)] (Mattaj, 1986; Plessel et al., 1994; Mouaikel et al., 2002) and subsequent import into the nucleus (Fischer et al., 1993). Within the nucleus, snRNPs are first targeted to Cajal bodies before moving to speckles. Additional modifications to the snRNAs (site-specific pseudouridylation and 2′-O-methylation) occur in Cajal bodies, and other specific proteins are added to the snRNPs (Jady et al., 2003). These modifications are mediated by small Cajal-body-specific RNAs called scaRNAs (Darzacq et al., 2002). The ongoing processes of snRNP modification and accumulation are possible triggers for Cajal body formation. Treatment with various transcription or nuclear export inhibitors causes Cajal body components to leave Cajal bodies (Carmo-Fonseca et al., 1992; Carvalho et al., 1999; Sleeman et al., 2001).

We previously performed a proteomic analysis of nuclear insoluble fractions to identify proteins involved in the

Journal of Cell Science

Journal of Cell Science

organization of nuclear structure (Takata et al., 2009). We then identified several factors that might be responsible for the nuclear architecture (Takata et al., 2009; Sharma et al., 2010). Several subunits of the integrator complex, a multiprotein mediator involved in 3′-end processing of snRNAs, were also identified in the nuclear insoluble fractions. Although the detailed mechanisms of the processing and its physiological implications remain unclear, an ongoing reaction in the nucleus (as for the integrator complex, the processing reaction of snRNA) is thought to be required for the formation of some nuclear structures. These observations raised concern about the relationship between the integrator complex and nuclear structure, and we therefore focused on the integrator complex in this study. Here, we show that without the activity of the integrator, Cajal body components, including coilin, SMN, Sm proteins and snRNAs disperse from Cajal bodies. Notably, SMN and Sm proteins accumulated at the cytoplasmic granules, and coilin at the nucleoli. These novel findings indicate that the integrity of Cajal bodies depends upon the integrator complex.

Results

INTS4 is required for the proper localization of coilin and SMN in Cajal bodies

Previously, we identified several integrator complex subunits from the nuclear insoluble fractions (Takata et al., 2009). To investigate complex function in nuclear organization, we performed RNAi-mediated depletion of integrator complex subunit 4 (INTS4) from HeLa cells using two different siRNAs. For control experiments, a non-targeting siRNA was used. The INTS4 protein level decreased by more than 80% within 60 hours after siRNA transfection (Fig. 1A). To determine the effects of knockdown of INTS4 on nuclear organization, we examined the localization of markers for various nuclear bodies, including nucleoli, nuclear speckles, nuclear envelope and Cajal bodies. We found severe coilin localization defects in Cajal bodies (Fig. 1B,C). Similar knockdown phenotypes were observed using both siRNAs. In 78% of control cells, coilin was detected in nuclear punctuate foci, which were presumably Cajal bodies (Fig. 1B,C). However, in INTS4-depleted cells, the

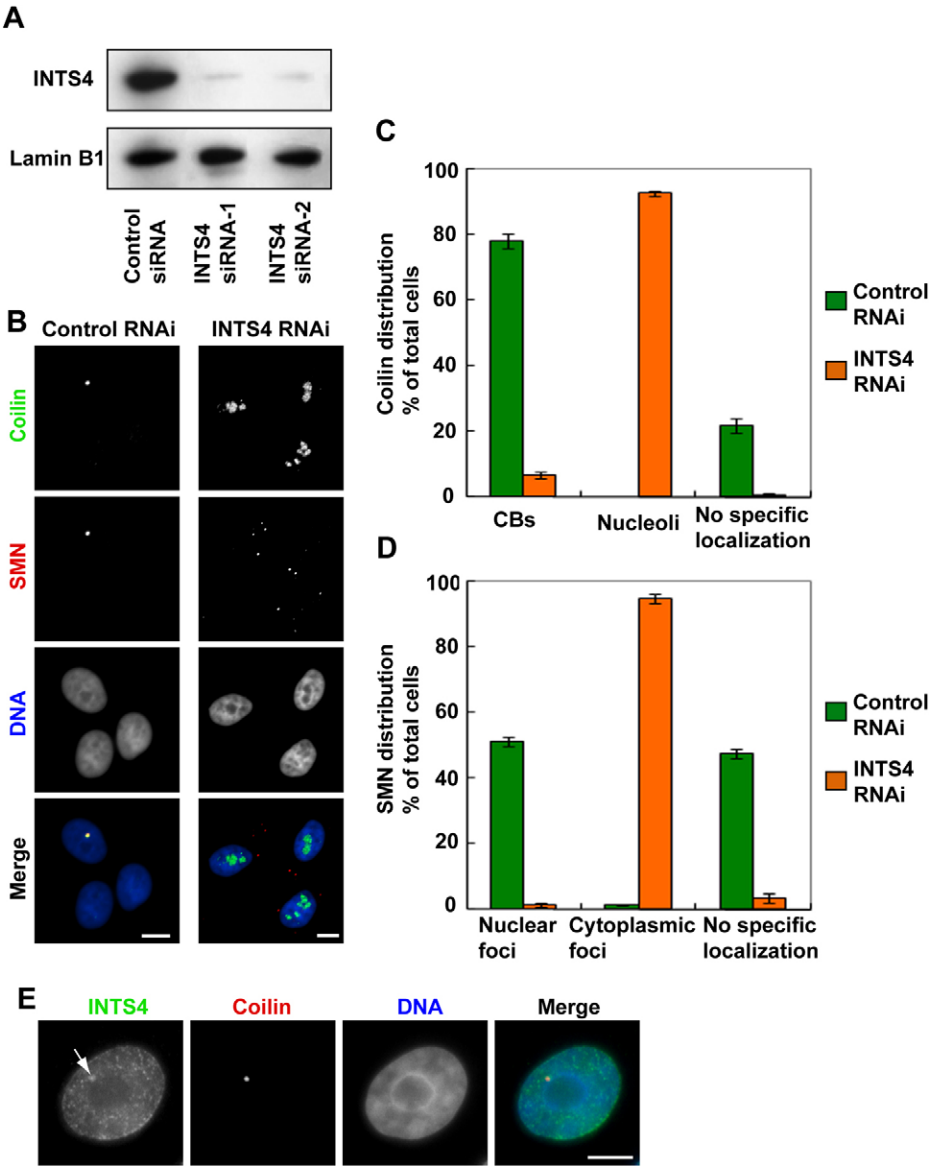

Fig. 1. Knockdown phenotype of INTS4. (**A**) HeLa cells were transfected with control siRNA, INTS4 siRNA-1 or INTS4 siRNA-2 and cultured for 60 hours. Cell extracts from RNAi-treated cells were separated using 12% SDS-polyacrylamide gels. INTS4 proteins were detected using an anti-INTS4 antibody. The amount of INTS4 decreased significantly in cells treated with siRNA-1 or siRNA-2 compared with control cells. Lamin B1 proteins were detected as internal controls. (**B**) INTS4-knockdown cells were fixed with 4% PFA and immunostained with anti-coilin antibody (green) and anti-SMN antibody (red); DNA was stained with DAPI (blue). Coilin is a marker protein for Cajal bodies. SMN is a component of the SMN complex and was localized in specific nuclear bodies, Gem or Cajal bodies in control cells. Scale bars: 10 μm. (**C**) Percentage coilin distribution in cells. Coilin localization patterns in control or INTS4-depleted cells were classified as in Cajal bodies, in nucleoli or with no specific localization. The values are means ± s.d. (error bars) of five independent experiments. More than 200 cells were counted in each experiment. (**D**) SMN distribution in cells. SMN localization patterns in control and INTS4-depleted cells were classified as nuclear foci, cytoplasmic granules or no specific localization. The values are means ± s.d. (error bars) of five independent experiments. More than 200 cells were counted in each experiment. (**E**) Localization of INTS4 (green) and coilin (red) in HeLa cells. DNA was stained with DAPI (blue). Arrow shows the INTS4 signals in Cajal bodies. Scale bar: 10 μm.

coilin signals strongly accumulated in the nucleoli, although some coilin fraction was still observed as faint foci in the nucleoplasm (Fig. 1B,C; supplementary material Fig. S1A). We called these faint nucleoplasmic foci of coilin 'immature Cajal-body-like structures'. The nucleolar accumulation of coilin was observed in 93% of INTS4-depleted cells (Fig. 1C). We also noticed prominent defects in SMN (gemin-1) localization in INTS4-depleted cells (Fig. 1B). SMN is known to localize to Cajal bodies and was detected as nuclear foci in 51% of control cells, whereas these nuclear foci were not visible in INTS4-depleted cells (Fig. 1B,D). Unexpectedly, SMN signals formed large cytoplasmic foci in 95% of INTS4-depleted cells. Thus, INTS4 depletion caused defects in the distribution of coilin and SMN. Additionally, 71.4% of coilin foci colocalized with INTS4 foci (Fig. 1E, arrow). These results suggest that INTS4 has a role in the integrity of Cajal bodies.

INTS4 is required for snRNP localization to Cajal bodies

We further investigated the localization of several other Cajal body components. In control RNAi cells, colocalization of Sm proteins and coilin was observed (Fig. 2A), indicating that some of the Sm proteins were indeed localized in Cajal bodies. However, this colocalization was not observed in INTS4-depleted cells. Moreover, similarly to SMN shown in Figure 1D, cytoplasmic foci of Sm proteins was clearly evident (Fig. 2A, arrow). We also observed colocalization of Sm proteins and SMN as granules in the cytoplasm of INTS4-depleted cells (supplementary material Fig. S1B, arrow). These cytoplasmic foci were rarely observed in control RNAi cells (1.6%), whereas 84% of the INTS4-depleted cells displayed these foci (Fig. 2C).

snRNAs normally form complexes with SMN and Sm proteins in the cytoplasm, and are trimethylated on their 5′-cap guanosine (TMG-capped). This complex is then transported into the

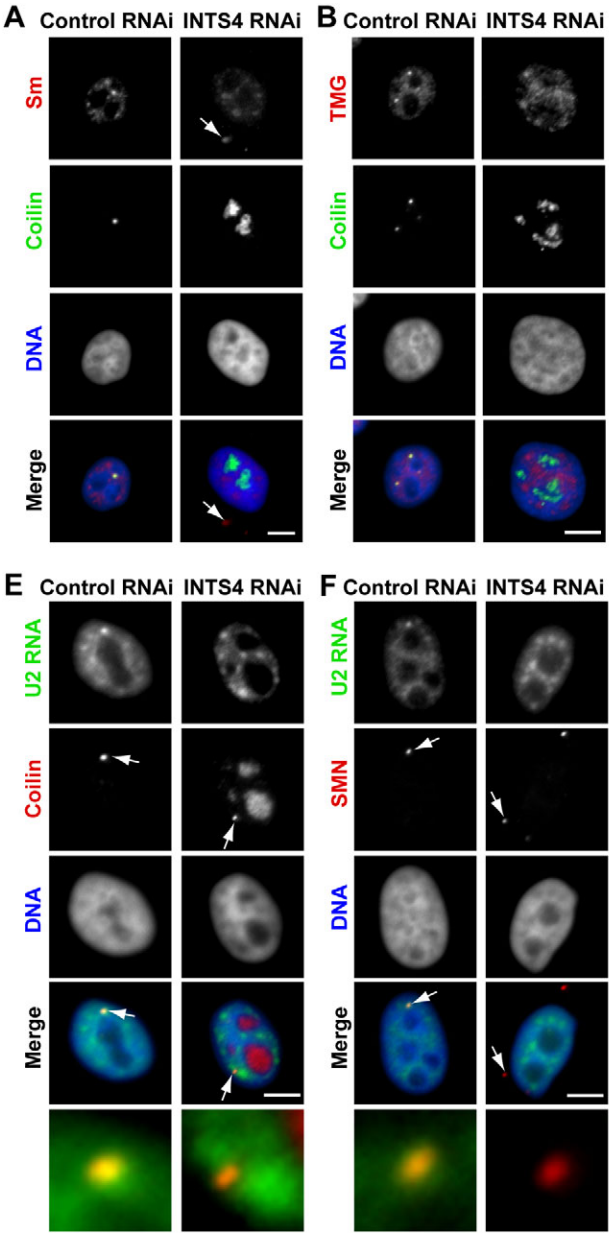

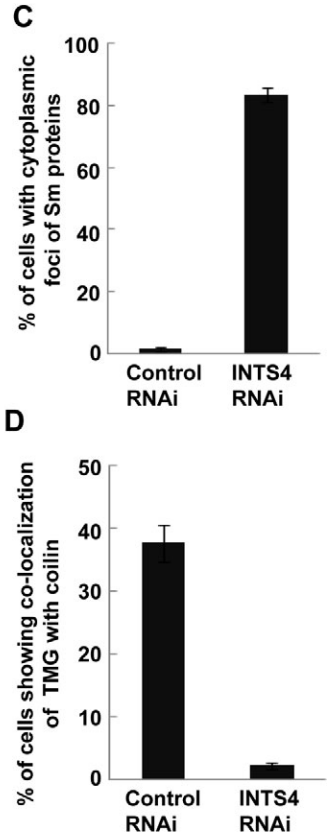

Fig. 2. Localization of Cajal body components in INTS4-knockdown cells. (**A**) Localization of Sm proteins in INTS4-depleted HeLa cells fixed with 4% PFA and double immunostained with anti-coilin antibody (green) and anti-Sm antibody (red). DNA was stained with DAPI (blue). Cytoplasmic foci of Sm proteins in INTS4-depleted cells are indicated by arrows. (**B**) Localization of TMG-capped RNAs in INTS4-depleted cells. TMG-capped RNA was detected using the anti-TMG antibody (red). Coilin (green) and DNA (blue) were also immunostained as in A. TMG-capped RNA signals were found in nucleoplasm and some of the signals were from Cajal bodies in which coilin was detected. However, this colocalization was diminished in INTS4-depleted cells. (**C**) Percentage of cells with cytoplasmic foci of Sm proteins. The values are means ± s.d. (error bars) of five independent experiments. More than 200 cells were counted in each experiment. (**D**) Percentage of cells showing colocalization of TMG-capped RNAs with coilin. The values are means ± s.d. (error bars) of five independent experiments. More than 200 cells were counted in each experiment. (**E**) RNA fluorescence in situ hybridization (FISH) of U2 snRNAs. U2 snRNAs were detected using U2 snRNA-specific probes (green) following immunostaining of coilin (red) to detect Cajal bodies. Enlarged images of the Cajal bodies indicated by arrows are also shown in the bottom panels. (**F**) Cytoplasmic granules did not contain snRNAs. U2 snRNAs were detected using U2 snRNA-specific probes (green) following immunostaining of SMN (red) to detect cytoplasmic foci of SMN proteins. Enlarged images of the SMN foci indicated by arrows are also shown in the bottom panels. Scale bars: 5 μm.

Journal of Cell Science

nucleus. Thus, the localization pattern of TMG-capped RNAs should be similar to that of Sm proteins. In Fig. 2B,D, 38% of control cells showed TMG signals colocalized with coilin in Cajal bodies; colocalization of TMG and Sm protein signals in the nuclei was also observed (supplementary material Fig. S1C). In the INTS4-depleted cells, the majority of coilin was delocalized to the nucleolus with a small amount of coilin remaining in the immature Cajal-body-like structures. Only 2% of the INTS4-depleted cells demonstrated colocalization of TMG-capped RNAs with coilin in the Cajal-body-like structures. Note that TMG signals were not detected in the cytoplasm (Fig. 2B) or in the cytoplasmic foci of Sm proteins (supplementary material Fig. S1C). This raised two possibilities: newly transcribed snRNAs are not hypermethylated in the cytoplasm and therefore could not be transported into the nucleus because the TMG cap is considered to be a nuclear localization signal (Fischer et al., 1993; Marshallsay and Luhrmann, 1994) or the snRNAs themselves are not located in the cytoplasm.

To test the possibilities above, we performed fluorescence in situ hybridization (FISH) using U2 snRNA probes. In control cells, U2 snRNAs localized mainly to Cajal bodies, with limited localization to nuclear speckles (Fig. 2E; supplementary material Fig. S1D). Unexpectedly, in INTS4-depleted cells, snRNA signals were not detected in the SMN cytoplasmic foci (Fig. 2F), indicating that SMN and Sm proteins form cytoplasmic structures without snRNAs. The snRNA signals were detected in the nucleus, but did not colocalize with coilin (Fig. 2E). This result implies that snRNPs do not localize to Cajal-body-like structures of INTS4-depleted cells. Immunofluorescent signals of Sm proteins and TMG-capped RNAs were still detected in nucleoplasmic regions other than Cajal bodies, both in control and INTS4-depleted cells. We suspect that these nucleoplasmic signals in INTS4-depleted cells were derived from pre-existing mature snRNPs before RNAi treatment because snRNPs are recycled within the nucleus and have long half-lives (Stanek et al., 2008).

INTS4-depleted cells show similar phenotypes to cells with inhibited nuclear snRNA export

Because the cytoplasmic structures observed in INTS4-depleted cells did not contain snRNAs, we suspected that newly transcribed snRNAs could not be exported into the cytoplasm. To test this possibility, we examined whether blocking snRNA export by depleting a phosphorylated adaptor for RNA export (PHAX) with specific siRNA or treating the cells with leptomycin B caused similar phenotypes as observed in INTS4-depleted cells. The efficient depletion of PHAX by RNAi was confirmed by western blotting (supplementary material Fig. S2). PHAX is required for snRNA export (Ohno et al., 2000). Leptomycin B is an inhibitor of CRM1-mediated nuclear export (Fornerod et al., 1997). When PHAX was depleted from HeLa cells, coilin accumulated in the nucleoli (Fig. 3A) (Lemm et al., 2006), as in the case of INTS4 depletion. Moreover, other Cajal body components (SMN, TMG and U2 snRNAs) disappeared from the Cajal-body-like structures (Fig. 3A–C). Cytoplasmic granules containing SMN were also observed in PHAX-depleted cells (Fig. 3A,C). After treating cells with leptomycin B, coilin accumulated in the nucleolus, SMN disappeared from Cajal-body-like structures and cytoplasmic granules containing SMN formed (Fig. 3D). Taken together, the effects of blocking snRNA export were similar to those observed upon depletion of INTS4. Furthermore, simultaneous depletion of INTS4 and PHAX, or leptomycin B treatment after INTS4 depletion, did not change the effects (Fig. 3E), suggesting that INTS4 functions in the same snRNA export pathway as PHAX and CRM1. These findings imply that INTS4 is associated with the export of snRNAs from the nucleus. This also explains why the SMN and Sm proteins are enriched in cytoplasmic granules and not imported into the nuclei in INTS4-depleted cells.

3′-End processing of snRNAs by the integrator complex is required for Cajal body integrity

Because INTS4 is a subunit of the integrator complex (Baillat et al., 2005), we next examined whether loss of integrator complex activity would cause the same phenotypes as seen in INTS4-depleted cells. We performed RNAi-mediated depletion of INTS11, which is a key subunit of the complex. INTS11 is essential for 3′-end processing of U2 snRNAs, and its depletion causes accumulation of U2 primary transcripts (Baillat et al., 2005). When INTS11 was depleted from HeLa cells, phenotypes similar to those found in INTS4-depleted cells were observed: coilin accumulated in the nucleoli and SMN formed foci in the cytoplasm (Fig. 4A,B). U2 snRNAs were not detected in Cajal-body-like structures (Fig. 4C). These results suggest that the phenotypes observed after INTS4 depletion were caused by defects in the integrator complex.

To test whether INTS4 is required for 3′-end processing of snRNAs in HeLa cells, we performed an RNase protection assay (RPA) of RNAs extracted from siRNA-treated cells using probes that recognize both mature and premature U2 snRNAs (Fig. 4D). As shown in Fig. 4E,F, the amount of premature U2 snRNAs in INTS4-depleted cells was more than twice that in control cells. This result shows that INTS4 is also required for 3′-end processing of snRNAs. Furthermore, these observations are consistent with a recent finding that INTS4 is required for U7 snRNA 3′-end formation in *Drosophila* (Ezzeddine et al., 2011). We also tested whether INTS4 is required for integrator complex formation by glycerol gradient sedimentation. In cells treated with control siRNA, INTS11 and INTS4 were detected in large molecular mass (~1 MDa) fractions (Fig. 4G). However, in INTS4-depleted cells, the INTS11 signal peaks in the high molecular mass fractions disappeared. This result indicates that INTS4 is required to form the integrator complex and that the 3′-end processing activity of snRNAs by this complex is essential for Cajal body integrity.

Cytoplasmic granule formation in INTS4-depleted cells

We observed that SMN and Sm proteins formed cytoplasmic granules without snRNAs in INTS4-depleted cells (Fig. 2F). What are these cytoplasmic granules? Similar cytoplasmic granules were observed by overexpressing SMN proteins (Hua and Zhou, 2004) and were thought to be ‘stress’ granules, which are organized in response to environmental stress (Anderson and Kedersha, 2009). We therefore performed immunostaining of T-cell internal antigen-1 (TIA-1), which is a stress granule marker protein (Kedersha and Anderson, 2007). TIA-1 was distributed diffusely in the nucleus and cytoplasm under normal culture conditions (Fig. 5A). When HeLa cells were incubated at 44℃, almost all of the cells formed stress granules containing TIA-1 (Fig. 5A, arrows). However, the cytoplasmic granules containing SMN upon knockdown of INTS4 did not contain TIA-1 (about

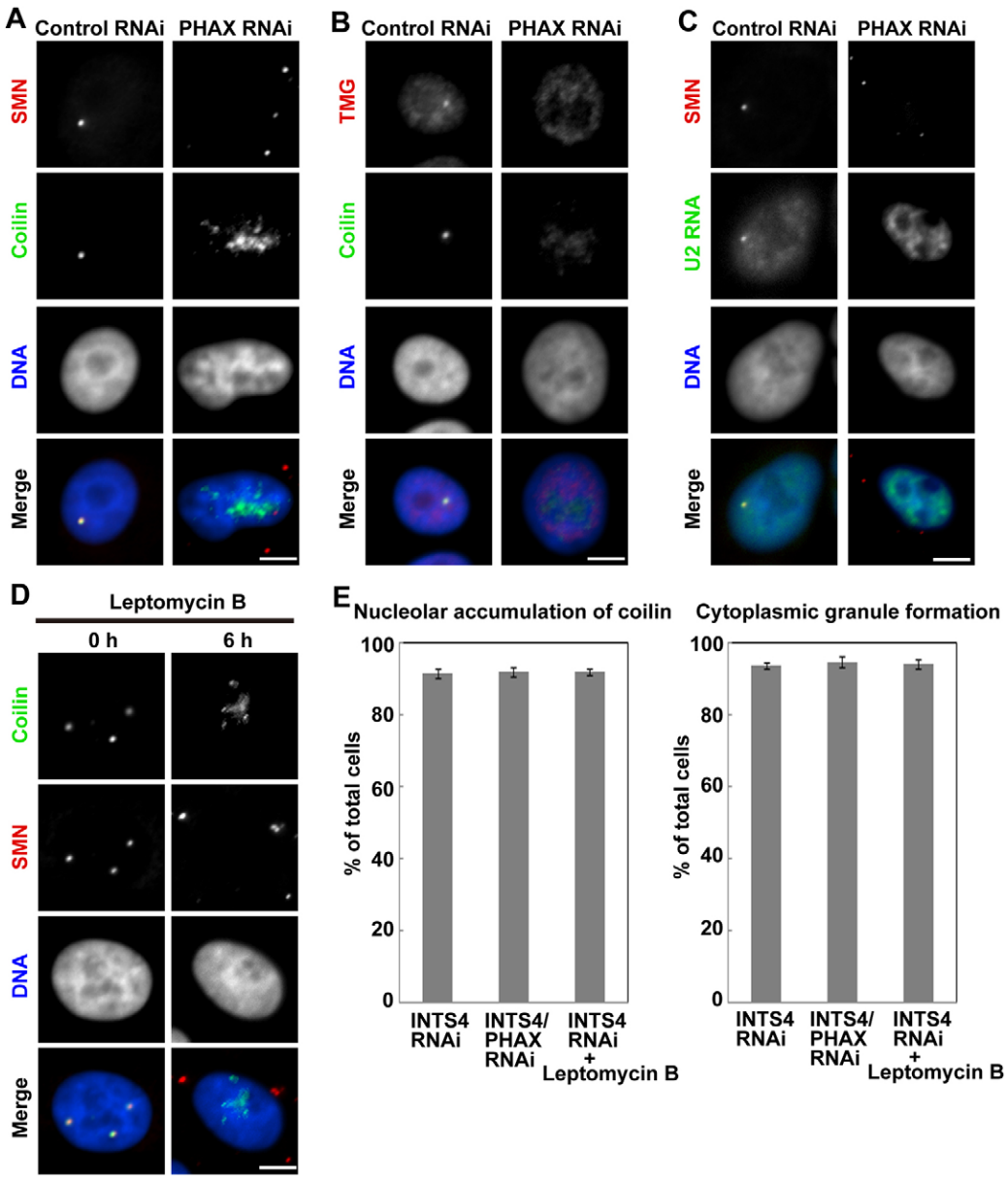

Fig. 3. Inhibition of snRNA export from the nucleus. (**A**–**C**) Localization of snRNP components in PHAX-depleted HeLa cells fixed with 4% PFA. (A) Coilin (green) and SMN (red), (B) coilin (green) and TMG-capped RNA (red), and (C) U2 snRNA (green) and SMN (red) were analyzed by double-immunostaining or immuno-FISH. DNA was stained with DAPI (blue). (**D**) HeLa cells were treated with 20 nM leptomycin B for 0 or 6 hours at 37℃, and coilin (green) and SMN (red) were detected by immunostaining. (**E**) Percentage of cells with nucleolar accumulation of coilin and cytoplasmic foci containing SMN in cells after INTS4 RNAi, INTS4 and PHAX RNAi, and INTS4 RNAi with leptomycin B treatment. The values are means ± s.d. (error bars) of five independent experiments. More than 200 cells were counted in each experiment. Scale bars: 5 μm.

1% of cells showed colocalization of SMN and TIA-1) (Fig. 5B), indicating that cytoplasmic granules are distinct from stress granules.

Another candidate for the cytoplasmic granules are U snRNP bodies (U bodies), in which snRNPs are assembled (Liu and Gall, 2007). U bodies were first discovered in ovarian cells of *Drosophila* and contain Cajal body components including SMN, Sm and snRNAs. U bodies were not prominent structures in HeLa cells (Fig. 1D), but we did observe them in the cytoplasm when a trimethylguanosine synthase (TGS1), required for hypermethylation of the 5′ cap of snRNAs, was depleted by RNAi (supplementary material Fig. S3). However, the cytoplasmic granules were different from U bodies because we could not detect U2 snRNA signals in the granules upon depletion of either INTS4 alone or both INTS4 and TGS1 (supplementary material Fig. S3).

How were the cytoplasmic granules formed upon INTS4 depletion? To address this question, we treated cells with RNase to examine the involvement of RNA in the cytoplasmic granules. As a result, RNA-dependent nuclear components, such as

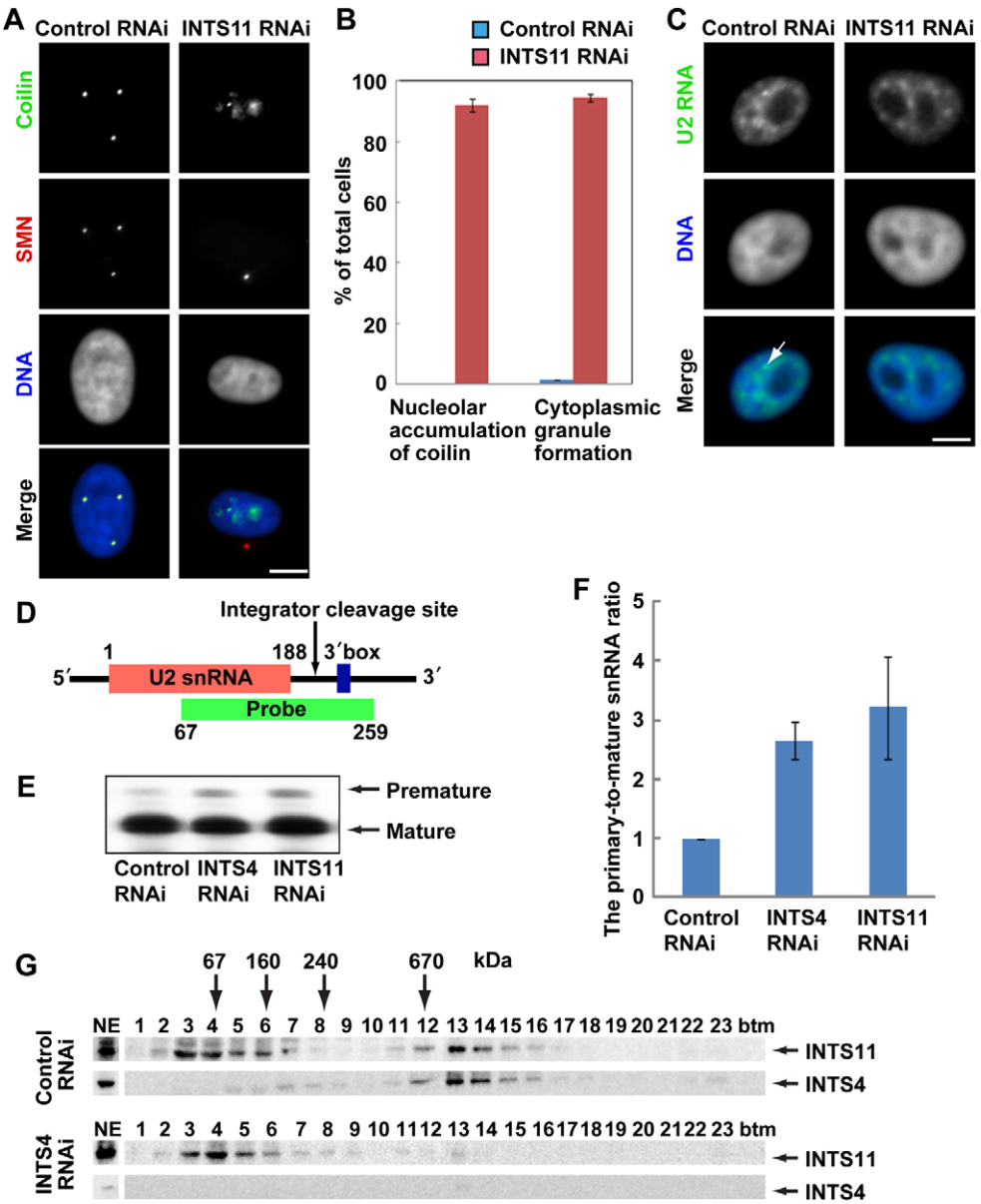

Fig. 4. Depletion of INTS11 produces a similar phenotype to that observed upon depletion of INTS4. (**A**) Effects of INTS11 knockdown on Cajal body components. INTS11-depleted HeLa cells were fixed with 4% PFA, and coilin (green) and SMN (red) were immunostained using their specific antibodies. (**B**) Percentage of cells with nucleolar accumulation of coilin and cytoplasmic granules containing SMN in control RNAi-treated cells and INTS4 RNAi-treated cells. The values are means ± s.d. (error bars) of five independent experiments. More than 200 cells were counted in each experiment. (**C**) RNA immuno-FISH of U2 snRNA (green) was performed on INTS11-depleted HeLa cells. Arrow indicates intense U2 snRNA signals in Cajal bodies. (**D**) The location of the RNA probe for premature U2 snRNA used in the RNA protection assay (RPA) is shown. The probe contains both mature and premature U2 snRNA sequences cleaved by the integrator. Numbers indicate the distance from the U2 snRNA start site (base). (**E**) RPA of U2 snRNAs extracted from cells after undergoing RNAi with control, INTS4 and INTS11 siRNA. Total RNA (10 µg) was analyzed using radiolabelled U2 snRNA probes. The band positions of premature U2 snRNAs and mature U2 snRNAs are indicated by arrows. (**F**) The primary to mature snRNA ratio in RNAi cells. The ratio was estimated by the intensity of the band for premature and mature U2 snRNAs shown in E (n=3; error bars represent the mean ± s.d.). (**G**) Fractionation of the integrator complex from nuclear extracts. Nuclear extracts (NEs) were prepared from HeLa cells treated with control or INTS4 siRNAi. The NEs were fractionated through a 20–50% glycerol gradient by centrifugation. The proteins in each fraction were separated on 12% SDS polyacrylamide gels, transferred to PVDF membrane and immunoblotted using anti-INTS11 and anti-INTS4 antibodies. Fraction numbers and the positions of molecular mass markers are indicated above each gel. Scale bars: 5 µm.

fibrillarin, nucleolin and TMG-capped RNAs, disappeared from the nucleus (supplementary material Fig. S4). However, the cytoplasmic granules containing SMN observed in INTS4-depleted cells were resistant to RNase treatment (Fig. 5C). Furthermore, the percentage of control cells containing cytoplasmic granules was unchanged by RNase treatment (Fig. 5D). These results suggest that cytoplasmic granule formation is independent of RNA.

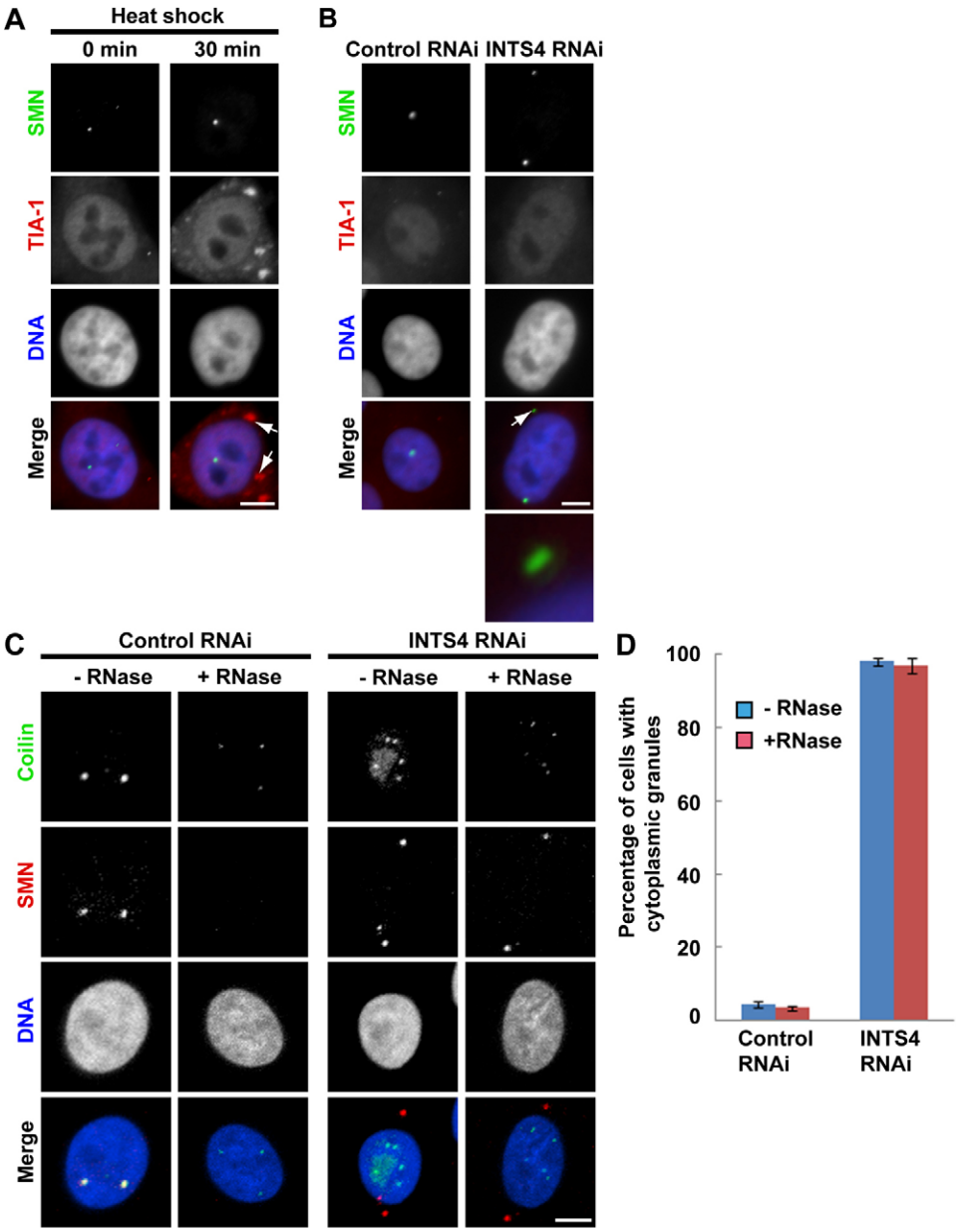

Fig. 5. Cytoplasmic structures induced by INTS4 depletion are not stress granules and are not sensitive to RNase. (**A**) Heat-shock treatment of HeLa cells. HeLa cells were incubated at 44℃ for 0 or 30 minutes and immunostained with anti-SMN antibody (green) and anti-TIA-1 antibody (red). DNA was stained with DAPI (blue). Arrows indicate stress granules. (**B**) Immunostaining of SMN (green) and TIA-1 (red) in siRNA-treated cells. An enlarged image of the cytoplasmic granules containing SMN indicated by a white arrow is also shown in the bottom panel. (**C**) HeLa cells were pre-extracted with cytoskeletal buffer containing 0.5% Triton X-100 and treated or not with RNase A. After fixation with 4% PFA, the cells were immunostained with anti-coilin antibody (green) and anti-SMN antibody (red). (**D**) Percentage of cells with cytoplasmic granules containing SMN with or without RNase treatments. The values are means ± s.d. (error bars) of four independent experiments. More than 200 cells were counted in each experiment. Scale bars: 5 μm.

Discussion

Cajal bodies are believed to be where mature snRNPs and snoRNPs are generated in the nucleus. However, the mechanism of Cajal body formation is not fully understood. In this study, we demonstrated that integrator complex activity is required for snRNP maturation and Cajal body integrity, as summarized in Fig. 6. Defects in the activity of the integrator complex abrogated the localization of Cajal body components (Fig. 2). 3′-Ends of the pre-snRNAs are processed by the integrator complex in the nucleus (Baillat et al., 2005). However, the biological significance of 3′-end processing of snRNAs is unclear. Our results suggest that snRNA processing is essential for their export. Although we do not know how 3′-end processing of the pre-snRNAs could contribute to their export, the 3′-end regions of the pre-snRNAs might destabilize the snRNA export complex unless the snRNAs are processed. Indeed, further 3′-end processing of snRNAs in the cytoplasm is required for nuclear re-import of snRNAs (Huang and Pederson, 1999). We propose that the 3′-end regions of snRNAs could function as an essential ‘code’ to determine their transport between the nucleus and cytoplasm (Fig. 6).

When either INTS4 or INTS11 was depleted, snRNPs disappeared from Cajal bodies and a small amount of coilin formed immature Cajal-body-like structures in the nucleoplasm. Additionally, SMN and Sm proteins formed bright foci in the cytoplasm (cytoplasmic granules), which were free of snRNAs. Formation of such cytoplasmic granules might be a common phenotype observed upon blocking snRNP assembly in the cytoplasm. Note that SMN and Sm proteins form cytoplasmic granules once overexpressed in HeLa cells (Sleeman et al., 2003). Expression of mutant SMN proteins blocking snRNP assembly in the cytoplasm is also reported to cause formation of similar

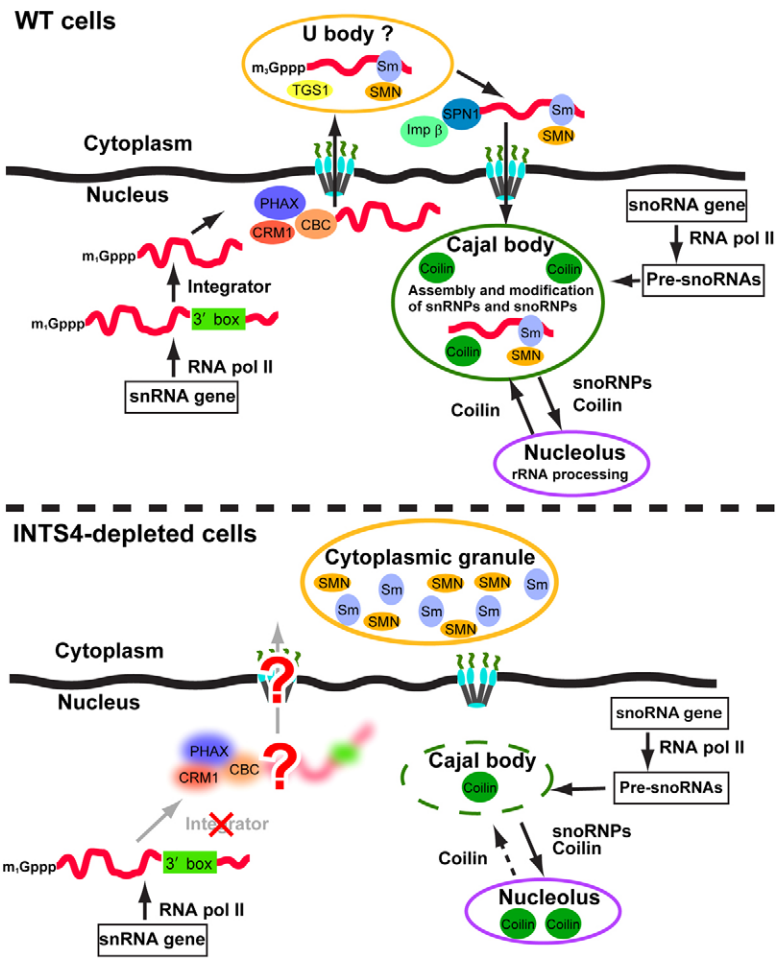

Fig. 6. Model of Cajal body formation. In wild-type cells, snRNAs are transcribed by RNA pol II and processed at the 3′-box by the integrator complex. snRNAs are exported from the nucleus by the CBC–PHAX–CRM1 complex. In the cytoplasm, Sm proteins bind to snRNAs with SMN proteins, and 5′ snRNA caps are hypermethylated by TGS1. These processes would occur in the U body, although the structure is not prominent in wild-type HeLa cell. The snRNPs are imported to the nucleus by SPN1 and importin-β. The snRNPs are further matured in the Cajal body and move to nuclear speckles. This flow of newly synthesized snRNPs is required for Cajal body integrity. Coilin moves between Cajal body and the nucleolus with snoRNPs. In INTS4-depleted cells, newly transcribed snRNAs are not processed at the 3′ box. Unprocessed snRNAs might cause defects in their export and induce accumulation of SMN and Sm proteins in the cytoplasm, although their relationship remains elusive. As newly synthesized snRNPs decrease in the nucleus, the Cajal body cannot maintain its integrity. The rate of movement of coilin toward Cajal body from the nucleolus decreases and coilin accumulates in the nucleolus in an RNA-dependent manner.

granules (Pellizzoni et al., 1998). These cytoplasmic granules did not contain TMG-capped snRNAs and coilin, like our observations in INTS-depleted cells.

We found a significant accumulation of coilin in nucleoli of INTS-knockdown cells. A similar phenotype was also seen previously upon loss of SMN protein or TGS1 (Shpargel and Matera, 2005; Girard et al., 2006; Lemm et al., 2006). How does coilin accumulate in nucleoli? Although we do not know the detailed mechanism, we suspect that some RNA molecules could be involved in the nucleolar accumulation because the accumulation was also observed by inhibiting snRNA transcription or snRNA export from the nucleus (Fig. 3; supplementary material Fig. S5) (Carmo-Fonseca et al., 1992). However, the coilin distribution patterns in the nucleolus differed between the two treatments. Transcriptional inhibition by actinomycin D caused coilin accumulation in a specific nucleolar body called the nucleolar cap (supplementary material Fig. S5) (Carmo-Fonseca et al., 1992). By contrast, inhibiting export with leptomycin B resulted in coilin accumulation in the whole nucleolus (supplementary material Fig. S5) (Carmo-Fonseca et al., 1992). The distribution of coilin observed in INTS-depleted cells was similar to that seen following leptomycin B treatment (supplementary material Fig. S5). Furthermore, we found that treating INTS4-depleted cells with actinomycin D resulted in a change in the localization of coilin to the nucleolar cap, whereas treatment with leptomycin B had no effect (supplementary material Fig. S5). This result suggests that coilin accumulation in the whole nucleolus arises from the generation of aberrant RNA molecules.

Consistent with this notion, coilin accumulation in the nucleolus disappeared following RNase treatment in INTS4-depleted cells (Fig. 5C). Thus, we suspected that snoRNPs are involved in coilin accumulation because they move between Cajal bodies and nucleoli (Gerbi et al., 2003). To test this possibility, we depleted fibrillarin, which is related to the maturation of snoRNPs (supplementary material Fig. S6). The results showed a decrease in the amount of snoRNAs in the nucleoli (supplementary material Fig. S6). In addition, simultaneous depletion of fibrillarin and INTS4 decreased the nucleolar accumulation of coilin correlated with the decrease of snoRNAs in the nucleoli (supplementary material Fig. S6). Aberrant snoRNPs, which might be generated by INTS depletion, would act to trap coilin in the nucleoli.

We previously identified the integrator complex, a multiprotein mediator of snRNA processing, from nuclear insoluble fractions (Takata et al., 2009). Our study here indicated that the activity of the integrator complex is essential for the integrity of Cajal bodies. An integrator was detected by chromatin immunoprecipitation at the U1 and U2 snRNA genes (Baillat et al., 2005), and colocalization of INTS4 and coilin was observed in the nucleus (Fig. 1E). Because the INTS4 subunit contains HEAT repeats, which are predicted to function as a flexible scaffold on which other proteins can be assembled, INTS4 might have a scaffold function to recruit coilin and

Journal of Cell Science

snRNPs to specific genomic regions, such as U snRNA gene loci and histone gene loci, where Cajal bodies often form (Frey and Matera, 1995; Smith et al., 1995; Shopland et al., 2001; Shevtsov and Dundr, 2011). Good examples of a flexible scaffold are condensin and cohesin complexes that play a dynamic role in packaging and shaping chromosomes (Neuwald and Hirano, 2000). Similarly to the role of condensin and cohesin in chromosome organization, INTS4 might aid the assembly of Cajal body components in addition to its original function as the integrator complex. Further study of INTS4 should elucidate the detailed mechanism of Cajal body formation in the nucleus.

Materials and Methods

Cell culture

Human HeLa cell lines were maintained in Dulbecco's modified Eagle's medium (Sigma) supplemented with 10% (v/v) fetal bovine serum (Nissui Seiyaku) and 2 mM L-glutamine (Sigma) at 37℃ under 5% CO_2 in air in a humidified incubator. For drug treatment, cells on coverslips were placed in fresh medium containing 5 μg/ml actinomycin D (Sigma) for 1 hour or 20 nM leptomycin B (Sigma) for 6 hours. For heat-shock experiments, cells on coverslips were incubated at 44℃ for 30 minutes in the prewarmed medium.

Antibodies

For immunofluorescence staining, the following primary antibodies were used at the indicated dilution: anti-coilin mouse monoclonal (P delta, Abcam) at 1:100; anti-coilin rabbit polyclonal (H-300, Santa Cruz Biotechnology) at 1:50; anti-SMN mouse monoclonal (2B1, Abcam) at 1:100; anti-Sm mouse monoclonal (Y12, Abcam) at 1:100; anti-Sm B/B′/N rabbit polyclonal (Santa Cruz Biotechnology) at 1:10; anti-2,2,7-trimethylguanosine (TMG) mouse monoclonal (K121, Calbiochem) at 1:100; anti-SC-35 mouse monoclonal (SC-35, Sigma) at 1:1000; anti-fibrillarin rabbit polyclonal (Abcam) at 1:100 and anti-TIA-1 goat polyclonal (C-20, Santa Cruz Biotechnology) at 1:50. The secondary antibodies, all used at a dilution of 1:200, were as follows: Alexa-Fluor-488-conjugated goat anti-rabbit IgG (Invitrogen); Alexa-Fluor-488-conjugated goat anti-mouse IgG (Invitrogen); Alexa-Fluor-488-conjugated donkey anti-mouse IgG (Invitrogen); Alexa-Fluor-546-conjugated donkey anti-goat IgG (Invitrogen); Alexa-Fluor-594-conjugated goat anti-rabbit IgG (Invitrogen) and TRITC-conjugated goat anti-mouse IgG (Sigma).

For immunoblotting, the following primary antibodies were used at the indicated dilution: anti-lamin-B1 rabbit polyclonal (Abcam) at 1:2000; anti-INTS4 rabbit polyclonal (Abcam) at 1:1000 and anti-INTS11 rabbit polyclonal (Abcam) at 1:2500. The secondary antibody, horseradish-peroxidase-linked anti-mouse IgG whole antibody (GE Healthcare), was used at a dilution of 1:40,000.

RNAi

The siRNAs used in this experiment were INTS4 siRNA-1 (5′-GCUAAAACC-UGUCCAACAATT-3′), INTS4 siRNA-2 (5′-AGAUACGUCUCAUGGUGUATT-3′), INTS3 siRNA (5′-GUGAUGGCAUGAAUAUUGTT-3′), INTS11 siRNA-2 (5′-UAACAGACUUCCUGGACUG-3′), fibrillarin siRNA (5′-GGAAUCAGUU-UAUGGAGAG-3′), TGS1 siRNA (5′-GAACAGAACUUCCUUAACA-3′) and PHAX siRNA (Boulon et al., 2004). The siRNAs were synthesized chemically and HeLa cells were transfected with 10 nM of siRNA duplexes using Lipofectamine RNAiMAX (Invitrogen) according to the manufacturer's instructions. For fibrillarin RNAi, we used 100 nM of siRNA duplexes. For control transfection, a control siRNA duplex, siGENOME Non-Targeting siRNA #2 (Dharmacon), was used. Cells were collected at 60 hours after transfection and used for further analysis.

Immunofluorescence localization of proteins

The cells on coverslips were fixed with 4% paraformaldehyde (PFA) for 10 minutes at 37℃ and permeabilized with 0.2% Triton X-100 in phosphate-buffered saline (PBS). For RNase treatment analysis, HeLa cells were pre-extracted with cytoskeletal buffer containing 0.5% Triton X-100 and treated with or without 1 mg/ml RNase A before fixation with 4% PFA. After incubation with 1% bovine serum albumin (BSA) in PBS for 30 minutes, the cells were incubated with primary antibodies for 1 hour at room temperature, followed by incubation with secondary antibodies for 1 hour. After washing, the cells were stained with 1 μg/ml DAPI and 1 μM TO-PRO-3 (Invitrogen). The samples were mounted using VECTASHIELD antifade mounting medium (Vector). Images were acquired using a Zeiss Axiovert 200M fluorescence microscope equipped with AxioCam HRm or a laser confocal microscope LSM 700 (Carl Zeiss Inc.) with a 40× objective lens (NA 0.75; Carl Zeiss). Images were acquired using Axiovision software (version 4.5; Carl Zeiss) or ZEN 2009 software (Carl Zeiss) and contrasted and merged using Photoshop (Adobe).

Fluorescence in situ hybridization

Cells grown on glass coverslips were washed with PBS and fixed with 4% PFA in PBS for 15 minutes at room temperature. After washing in PBS, cells were permeabilized with 0.2% Triton X-100 in PBS on ice for 5 min and were washed twice with PBS and with 2× standard saline citrate (SSC) buffer/50% formamide for 5 minutes. Oligonucleotide probes against U1 and U2 snRNAs and U3 snoRNA were synthesized chemically and labeled at the 5′-end with Alexa Fluor 488. The sequences of the probes were as follows: U1 snRNA, 5′-CCGGAGTGCAATGGATAAGCCTCGCCCTGGG-3′; U2 snRNA, 5′-GA-ACAGATACTACACTTGATCTTAGCCAAAAGGCCGAGAAGC-3′; and U3 snoRNA, 5′-GTTCTCTCCCTCTCACTCCCCAATACGGAGAGAAGAACGATCA-TCAATGGCTG-3′. The hybridization mixture was prepared using 1 μg of oligonucleotide probe against snRNAs or snoRNAs and 50 μg yeast tRNA per coverslip and was made to a final concentration of 2× SSC, 20% formamide and 10% dextran sulfate. A hybridization mixture was placed onto each coverslip, and the coverslips were sealed onto glass microscope slides using rubber cement and allowed to incubate in a water chamber overnight at 37℃. The coverslips were washed with 2× SSC and 50% formamide at 37℃ for 5 minutes, with 0.2% Tween20 in 4× SSC at room temperature for 5 minutes and finally with PBS at room temperature for 5 minutes. The coverslips were mounted in VECTASHIELD antifade mounting medium with 1 μg/ml DAPI.

Cell extraction and density gradient sedimentation

Cell extraction was carried out as described previously (Baillat et al., 2005) with the following modifications. Harvested cells were swollen in two volumes of hypotonic buffer (10 mM Tris-HCl, pH 8.0, 5 mM KCl, 1.5 mM $MgCl_2$, 1.0 mM DTT) containing protease inhibitors (PMSF, pepstatin A, leupeptin, aprotinin and benzamidine). Cells were homogenized using a Dounce homogenizer, and centrifuged at 780 ***g*** for 5 minutes to separate the nuclei pellet fraction. Washed nuclei ware suspended in nuclear extraction buffer (20 mM Tris-HCl, pH 8.0, 10% glycerol, 300 mM KCl, 1.5 mM $MgCl_2$, 1.0 mM EDTA, 1.0 mM DTT, 0.1% NP-40) containing protease inhibitors, homogenized, and followed by incubation at 4℃ for 30 minutes. After centrifugation at 100,000 ***g*** for 60 minutes, supernatants were used as extracts of nuclear fractions. Nuclear extracts (0.2 ml) loaded onto a surface of 5 ml of 20–50% glycerol gradient (20 mM Tris-HCl, pH 8.0, 300 mM KCl, 1.5 mM $MgCl_2$), and centrifuged at 240,000 ***g*** in swing rotor at 4℃ for 12 hours. About 22 fractions (~200 μl) were collected from the top of tube by using piston gradient fractionator (BioComp Instrument). Each fraction was precipitated with 20% TCA, followed by SDS-PAGE and western blotting analyses. All experiments were conducted with a parallel gradient for the marker proteins Thyroglobulin (670 kDa), catalase (232 kDa), aldolase (158 kDa), BSA (66 kDa) and lysozyme (14 kDa).

Immunoblotting

Ten-microgram aliquots of proteins from RNAi-treated HeLa cells were separated on 12% polyacrylamide gels and transferred to polyvinylidene fluoride (PVDF) membranes (Millipore) at 70 V for 3 hours. After incubation with 4% BSA in TBS-T for 1 hour, the membrane was incubated with primary antibodies for 1 hour at room temperature, followed by incubation with secondary antibodies for 1 hour. Signals were detected using SuperSignal West Femto Maximum Sensitivity Substrate (Thermo Scientific).

RNase protection assay

Total RNAs were extracted from siRNA-treated HeLa cells using TRIzol reagent (Invitrogen). For RNA probe synthesis, the 3′ half of the U2 snRNA gene was amplified from HeLa genomic DNA by polymerase chain reaction (PCR) using the synthetic primers 5′-CGTCCTCTATCCGAGGACAAT-3′ and 5′-CAAGCCGC-CCCGCAGGTGCTAC-3′. PCR products were cloned into the pPCR-Script Amp SK(+) cloning vector (Stratagene). RNA probes, labeled with [α-^{32}P]CTP, were transcribed using In vitro Transcription T7 kits (Takara Bio) from template plasmids linearized using *Not*I, constructed as described above. The transcribed RNA probes were purified by DNase I digestion, phenol–chloroform–isoamyl-alcohol extraction and ethanol precipitation. Total RNAs (10 μg) were hybridized with RNA probes overnight at 45℃. Probe excess was confirmed with twofold amounts of total RNA (data not shown). The hybridized RNAs were digested with 20 U RNase T1 for 30 minutes at 30℃ (Takara Bio). After digestion with 50 μg of proteinase K for 15 minutes at 50℃, the ribonuclease-resistant products were extracted with phenol–chloroform–isoamyl-alcohol, precipitated with ethanol and then resolved by 6% polyacrylamide and 8 M urea gel electrophoresis, followed by autoradiography.

Acknowledgements

We would like to thank T. Tani (Kumamoto University), N. Saitoh (Kumamoto University) and K. Fujimura (University of Tokyo) for their critical reading of this manuscript. We also thank T. Ono, T. Sakaguchi and K. Takagi for helpful discussion, and we deeply

appreciate A. Morohoshi, N. Nobe, Y. Wakata, K. Kunita, M. Hara and N. Takeyama for technical assistance.

Funding

This work was supported in part by a Grant-in-Aid for Scientific Research on Priority Areas and City Area Program from the Japanese Ministry of Education, Culture, Sports, Science and Technology (MEXT) and grants from the Transdisciplinary Research Integration Center, Research Organization of Information and Systems, the Seed Of Excellence Foundation in Shizuoka Prefecture, the Takeda Science Foundation and the Naito Foundation, Japan. HT is a research fellow of the Japan Society for the Promotion of Science.

Supplementary material available online at
http://jcs.biologists.org/lookup/suppl/doi:10.1242/jcs.090837/-/DC1

References

Anderson, P. and Kedersha, N. (2009). RNA granules: post-transcriptional and epigenetic modulators of gene expression. *Nat. Rev. Mol. Cell Biol.* **10**, 430-436.

Baillat, D., Hakimi, M. A., Naar, A. M., Shilatifard, A., Cooch, N. and Shiekhattar, R. (2005). Integrator, a multiprotein mediator of small nuclear RNA processing, associates with the C-terminal repeat of RNA polymerase II. *Cell* **123**, 265-276.

Beven, A. F., Simpson, G. G., Brown, J. W. and Shaw, P. J. (1995). The organization of spliceosomal components in the nuclei of higher plants. *J. Cell Sci.* **108**, 509-518.

Boulon, S., Verheggen, C., Jady, B. E., Girard, C., Pescia, C., Paul, C., Ospina, J. K., Kiss, T., Matera, A. G., Bordonne, R. et al. (2004). PHAX and CRM1 are required sequentially to transport U3 snoRNA to nucleoli. *Mol. Cell* **16**, 777-787.

Cajal, S. R. (1903). Un sencillo metodo de coloracion selectiva del reticulo protoplasmatico y sus efectos en los diversos organos nerviosos de vertebrados e invertebrados. *Trab. Lab. Invest. Biol.* **2**, 129-221.

Carmo-Fonseca, M., Pepperkok, R., Carvalho, M. T. and Lamond, A. I. (1992). Transcription-dependent colocalization of the U1, U2, U4/U6, and U5 snRNPs in coiled bodies. *J. Cell Biol.* **117**, 1-14.

Carvalho, T., Almeida, F., Calapez, A., Lafarga, M., Berciano, M. T. and Carmo-Fonseca, M. (1999). The spinal muscular atrophy disease gene product, SMN: A link between snRNP biogenesis and the Cajal (coiled) body. *J. Cell Biol.* **147**, 715-728.

Cioce, M. and Lamond, A. I. (2005). Cajal bodies: a long history of discovery. *Annu. Rev. Cell Dev. Biol.* **21**, 105-131.

Cremer, T., Cremer, M., Dietzel, S., Muller, S., Solovei, I. and Fakan, S. (2006). Chromosome territories – a functional nuclear landscape. *Curr. Opin. Cell Biol.* **18**, 307-316.

Darzacq, X., Jady, B. E., Verheggen, C., Kiss, A. M., Bertrand, E. and Kiss, T. (2002). Cajal body-specific small nuclear RNAs: a novel class of 2′-O-methylation and pseudouridylation guide RNAs. *EMBO J.* **21**, 2746-2756.

Ezzeddine, N., Chen, J., Waltenspiel, B., Burch, B., Albrecht, T., Zhuo, M., Warren, W. D., Marzluff, W. F. and Wagner, E. J. (2011). A subset of Drosophila integrator proteins is essential for efficient U7 snRNA and spliceosomal snRNA 3′-end formation. *Mol. Cell Biol.* **31**, 328-341.

Fischer, U., Sumpter, V., Sekine, M., Satoh, T. and Luhrmann, R. (1993). Nucleo-cytoplasmic transport of U snRNPs: definition of a nuclear location signal in the Sm core domain that binds a transport receptor independently of the m3G cap. *EMBO J.* **12**, 573-583.

Fornerod, M., Ohno, M., Yoshida, M. and Mattaj, I. W. (1997). CRM1 is an export receptor for leucine-rich nuclear export signals. *Cell* **90**, 1051-1060.

Frey, M. R. and Matera, A. G. (1995). Coiled bodies contain U7 small nuclear RNA and associate with specific DNA sequences in interphase human cells. *Proc. Natl. Acad. Sci. USA* **92**, 5915-5919.

Gall, J. G. (2000). Cajal bodies: the first 100 years. *Annu. Rev. Cell Dev. Biol.* **16**, 273-300.

Gerbi, S. A., Borovjagin, A. V. and Lange, T. S. (2003). The nucleolus: a site of ribonucleoprotein maturation. *Curr. Opin. Cell Biol.* **15**, 318-325.

Girard, C., Neel, H., Bertrand, E. and Bordonne, R. (2006). Depletion of SMN by RNA interference in HeLa cells induces defects in Cajal body formation. *Nucleic Acids Res.* **34**, 2925-2932.

Hua, Y. and Zhou, J. (2004). Survival motor neuron protein facilitates assembly of stress granules. *FEBS Lett.* **572**, 69-74.

Huang, Q. and Pederson, T. (1999). A human U2 RNA mutant stalled in 3′ end processing is impaired in nuclear import. *Nucleic Acids Res.* **27**, 1025-1031.

Huang, Q., Jacobson, M. R. and Pederson, T. (1997). 3′ processing of human pre-U2 small nuclear RNA: a base-pairing interaction between the 3′ extension of the precursor and an internal region. *Mol. Cell Biol.* **17**, 7178-7185.

Jady, B. E., Darzacq, X., Tucker, K. E., Matera, A. G., Bertrand, E. and Kiss, T. (2003). Modification of Sm small nuclear RNAs occurs in the nucleoplasmic Cajal body following import from the cytoplasm. *EMBO J.* **22**, 1878-1888.

Kaiser, T. E., Intine, R. V. and Dundr, M. (2008). De novo formation of a subnuclear body. *Science* **322**, 1713-1717.

Kedersha, N. and Anderson, P. (2007). Mammalian stress granules and processing bodies. *Methods Enzymol.* **431**, 61-81.

Kolb, S. J., Battle, D. J. and Dreyfuss, G. (2007). Molecular functions of the SMN complex. *J. Child Neurol.* **22**, 990-994.

Lamond, A. I. and Earnshaw, W. C. (1998). Structure and function in the nucleus. *Science* **280**, 547-553.

Lemm, I., Girard, C., Kuhn, A. N., Watkins, N. J., Schneider, M., Bordonne, R. and Luhrmann, R. (2006). Ongoing U snRNP biogenesis is required for the integrity of Cajal bodies. *Mol. Biol. Cell* **17**, 3221-3231.

Liu, J. L. and Gall, J. G. (2007). U bodies are cytoplasmic structures that contain uridine-rich small nuclear ribonucleoproteins and associate with P bodies. *Proc. Natl. Acad. Sci. USA* **104**, 11655-11659.

Marshallsay, C. and Luhrmann, R. (1994). In vitro nuclear import of snRNPs: cytosolic factors mediate m3G-cap dependence of U1 and U2 snRNP transport. *EMBO J.* **13**, 222-231.

Matera, A. G. and Shpargel, K. B. (2006). Pumping RNA: nuclear bodybuilding along the RNP pipeline. *Curr. Opin. Cell Biol.* **18**, 317-324.

Mattaj, I. W. (1986). Cap trimethylation of U snRNA is cytoplasmic and dependent on U snRNP protein binding. *Cell* **46**, 905-911.

Misteli, T. (2007). Beyond the sequence: cellular organization of genome function. *Cell* **128**, 787-800.

Mouaikel, J., Verheggen, C., Bertrand, E., Tazi, J. and Bordonne, R. (2002). Hypermethylation of the cap structure of both yeast snRNAs and snoRNAs requires a conserved methyltransferase that is localized to the nucleolus. *Mol. Cell* **9**, 891-901.

Neuwald, A. F. and Hirano, T. (2000). HEAT repeats associated with condensins, cohesins, and other complexes involved in chromosome-related functions. *Genome Res.* **10**, 1445-1452.

Ogg, S. C. and Lamond, A. I. (2002). Cajal bodies and coilin – moving towards function. *J. Cell Biol.* **159**, 17-21.

Ohno, M., Segref, A., Bachi, A., Wilm, M. and Mattaj, I. W. (2000). PHAX, a mediator of U snRNA nuclear export whose activity is regulated by phosphorylation. *Cell* **101**, 187-198.

Pellizzoni, L., Kataoka, N., Charroux, B. and Dreyfuss, G. (1998). A novel function for SMN, the spinal muscular atrophy disease gene product, in pre-mRNA splicing. *Cell* **95**, 615-624.

Plessel, G., Fischer, U. and Luhrmann, R. (1994). m3G cap hypermethylation of U1 small nuclear ribonucleoprotein (snRNP) in vitro: evidence that the U1 small nuclear RNA-(guanosine-N2)-methyltransferase is a non-snRNP cytoplasmic protein that requires a binding site on the Sm core domain. *Mol. Cell Biol.* **14**, 4160-4172.

Raker, V. A., Plessel, G. and Luhrmann, R. (1996). The snRNP core assembly pathway: identification of stable core protein heteromeric complexes and an snRNP subcore particle in vitro. *EMBO J.* **15**, 2256-2269.

Sharma, A., Takata, H., Shibahara, K., Bubulya, A. and Bubulya, P. A. (2010). Son is essential for nuclear speckle organization and cell cycle progression. *Mol. Biol. Cell* **21**, 650-663.

Shevtsov, S. P. and Dundr, M. (2011). Nucleation of nuclear bodies by RNA. *Nat. Cell Biol.* **13**, 167-173.

Shopland, L. S., Byron, M., Stein, J. L., Lian, J. B., Stein, G. S. and Lawrence, J. B. (2001). Replication-dependent histone gene expression is related to Cajal body (CB) association but does not require sustained CB contact. *Mol. Biol. Cell* **12**, 565-576.

Shpargel, K. B. and Matera, A. G. (2005). Gemin proteins are required for efficient assembly of Sm-class ribonucleoproteins. *Proc. Natl. Acad. Sci. USA* **102**, 17372-17377.

Sleeman, J. E. and Lamond, A. I. (1999). Newly assembled snRNPs associate with coiled bodies before speckles, suggesting a nuclear snRNP maturation pathway. *Curr. Biol.* **9**, 1065-1074.

Sleeman, J. E., Ajuh, P. and Lamond, A. I. (2001). snRNP protein expression enhances the formation of Cajal bodies containing p80-coilin and SMN. *J. Cell Sci.* **114**, 4407-4419.

Sleeman, J. E., Trinkle-Mulcahy, L., Prescott, A. R., Ogg, S. C. and Lamond, A. I. (2003). Cajal body proteins SMN and Coilin show differential dynamic behaviour in vivo. *J. Cell Sci.* **116**, 2039-2050.

Smith, K. P., Carter, K. C., Johnson, C. V. and Lawrence, J. B. (1995). U2 and U1 snRNA gene loci associate with coiled bodies. *J. Cell Biochem.* **59**, 473-485.

Stanek, D., Pridalova-Hnilicova, J., Novotny, I., Huranova, M., Blazikova, M., Wen, X., Sapra, A. K. and Neugebauer, K. M. (2008). Spliceosomal small nuclear ribonucleoprotein particles repeatedly cycle through Cajal bodies. *Mol. Biol. Cell* **19**, 2534-2543.

Takata, H., Nishijima, H., Ogura, S., Sakaguchi, T., Bubulya, P. A., Mochizuki, T. and Shibahara, K. (2009). Proteome analysis of human nuclear insoluble fractions. *Genes Cells* **14**, 975-990.

Zhao, R., Bodnar, M. S. and Spector, D. L. (2009). Nuclear neighborhoods and gene expression. *Curr. Opin. Genet. Dev.* **19**, 172-179.